water

MDPI

Article

Variations of Stable Isotopes in Daily Precipitation in a Monsoon Region

Jie Li [1,2], Zhonghe Pang [2,3,4,*], Lijun Tian [5], Hongyi Zhao [6] and Guoying Bai [6]

1 Engineering Research Center of Groundwater Pollution Control and Remediation, Ministry of Education, College of Water Sciences, Beijing Normal University, Beijing 100875, China
2 Key Laboratory of Shale Gas and Geoengineering, Institute of Geology and Geophysics, Chinese Academy of Sciences, Beijing 100029, China
3 Institutions of Earth Science, Chinese Academy of Sciences, Beijing 100029, China
4 University of Chinese Academy of Sciences, Beijing 100049, China
5 Key Laboratory of Cenozoic Geology and Environment, Institute of Geology and Geophysics, Chinese Academy of Sciences, Beijing 100029, China
6 Beijing Hydrological Center, Beijing 100089, China
* Correspondence: z.pang@mail.iggcas.ac.cn

Abstract: The stable isotopes of hydrogen and oxygen in precipitation provide a useful reference for the study of hydrological processes, but concerns have been raised regarding the established patterns in their variations in a monsoon climate zone. In this study, stable isotopes ($\delta^{18}O$ and $\delta^{2}H$) of 539 daily precipitation samples from seven hydrometeorological stations in the Beijing area were used to investigate short-term isotopic variations and the controlling factors at a region with a monsoon climate. The $\delta^{18}O$ in the precipitation increases from the northwest to the south, which is controlled by the monsoon from the south and continental moisture from the northwest. Consistently, both the high $\delta^{18}O$ values and low deuterium excess values from May to September reveal the impact of the monsoon. The amount effect is significant during the monsoon season. In contrast, the T effect is significant, with a gradient of 0.4‰ per °C during the non-monsoon season. A Rayleigh distillation model indicates that the moisture source and residual vapor fraction are the two most important factors in controlling the $\delta^{18}O$ patterns in precipitation in a monsoon region, independent of temperature. The result of this study is helpful for the understanding of the regional atmospheric water cycle.

Keywords: stable isotopes; daily precipitation; monsoon; isotopic effects; BNIP

check for updates

Citation: Li, J.; Pang, Z.; Tian, L.; Zhao, H.; Bai, G. Variations of Stable Isotopes in Daily Precipitation in a Monsoon Region. *Water* **2022**, *14*, 2891. https://doi.org/10.3390/w14182891

Academic Editor: Paolo Madonia

Received: 24 July 2022
Accepted: 10 September 2022
Published: 16 September 2022

1. Introduction

Stable isotope records of paleo-precipitation preserved in the natural archives (e.g., speleothems, tree rings, ice cores, corals, and lake/ocean sediments) have provided information on past climate change at the regional and global scales [1–4] with the assumption that the $\delta^{18}O$ of the archives ($\delta^{18}O_a$) follows the changes of precipitation $\delta^{18}O$ ($\delta^{18}O_p$) [5–7]. However, the climatic significance of $\delta^{18}O_a$ remains a debate. For example, depleted $\delta^{18}O$ in groundwater ($\delta^{18}O_g$) was reported for the late Pleistocene groundwater in North China and West Africa, which was attributed to temperature changes [8–11] or monsoon strength [12]. The enriched stalagmite $\delta^{18}O$ ($\delta^{18}O_s$) from monsoon regions was observed in the late Pleistocene, as a proxy of the local rainfall amount [13–15], or variations in monsoon intensity [3,16–18], or changes in moisture sources [19–23]. Furthermore, some studies emphasized that $\delta^{18}O_s$ and $\delta^{18}O_g$ are biased to the heavy rain events during the wet season [24–29].

Resolving these debates requires a good understanding of the isotopic composition of precipitation. Numerous studies have investigated precipitation isotopes, especially the relationship between T or P and isotopes [30–32]. Araguas-Araguas et al. (1998) [33]

analyzed the stable isotope composition of precipitation over Southeast Asia and concluded that $\delta^{18}O_P$ values increase with T in the north and decrease with P in the south. Subsequently, Johnson and Ingram (2004) [34] demonstrated that the multiple regression method should be used rather than the traditional single regression method with only T or P. Li et al. (2014) [31] further detailed a strong positive relationship between $\delta^{18}O_P$ and T in winter, and a negative linear correlation between $\delta^{18}O_P$ and summer P. Tan (2014) [35] found that $\delta^{18}O_P$ reflects neither the amount effect nor strength of a single summer monsoon, but the intensity contrast between two summer monsoons: the southwest and southeast monsoons in the monsoon regions of China. The stable isotope systematics are quite complex in the monsoon-affected regions of China, and thus further work should be completed with higher resolution data. In recent years, event precipitation and even intra-event sampling for isotopic analysis have been carried out in order to gain insight into the complex processes/factors controlling precipitation isotopes [36–38]. Li et al. (2015) [39] identified different moisture sources dominating the variations in precipitation isotopes during an extreme event in Beijing. Although a great deal of work is related to stable isotopes in precipitation, little attention has been paid to the contributions of non-monsoon precipitation in the monsoon margin area.

Here, we argue that high-resolution data from both the temporal and spatial sampling of precipitation events can provide more information on the factors and processes controlling the variations in modern precipitation isotopes. The Beijing region, the northern extent of the East Asian summer monsoon (EASM) in northern China, was selected as a study area. We established a daily precipitation event sampling network with a spatial resolution of one station every 2500 km^2, covering the mountains and plains over the Beijing region. Based on the observation throughout 2015, the primary objectives of this study include: (1) Do moisture sources, moisture trajectories, and/or local metrological conditions control the isotopic variations of precipitation? (2) What is the relationship between precipitation isotope and T or P at the eventful, seasonal, and annual scales?

2. Data and Methods

2.1. Study Area

Beijing, the capital of China, is in the northern rim of the North China Plain (Figure 1a). Due to the typical continental monsoon climate, there are four distinct seasons in Beijing. The non-monsoon season is cold and dry, due to northerly winds blowing from high-latitude areas, while the monsoon season is hot and wet because of the east and south airflow carrying moisture from the southern Pacific Ocean and Indian Ocean [40,41]. The annual precipitation is 574 mm, of which 70% occurs during the monsoonal season from May to September (Figure 1b,c). The average annual temperature is approximately 12 °C. The mean air temperature in the mountain area is lower (10.2 °C at YQ station) than that in the plains (15.1 °C at BTC station).

2.2. Sampling and Analysis

To better characterize the moisture circulation over the Beijing area, we established the Beijing Network of Isotopes in Precipitation (BNIP) based on the principal hydrologic stations of the Beijing Water Authority in May 2014 (Figure 1). A rain collector composed of a polyethylene bottle and funnel was placed outside at each station, with a ping-pong ball placed at the funnel mouth to prevent evaporation. Snow samples were collected using a pail installed on the ground. After each snowfall event, snow samples were melted at room temperature. The precipitation samples were collected at 8:00 am in the next day after the precipitation events. Samples were immediately sealed after collection in 20 mL fully filled bottles to avoid evaporation after rainfall, and then transported to the laboratory and stored at 4 °C until the analysis. Stable isotopes were analyzed on a Picarro L1102-i Laser Absorption Water Isotope Spectrometer at the Water Isotope and Water–Rock Interaction Laboratory, Institute of Geology and Geophysics, Chinese Academy of Sciences. Results were reported as $\delta^{18}O$ ($\delta^{18}O = (R_{sample}/R_{standard} - 1) \times 1000$) using the Vienna Standard

Mean Ocean Water (VSMOW) standard. The analytical precisions for δ^2H and $\delta^{18}O$ were 0.5‰ and 0.1‰, respectively. Meteorological variables, including precipitation amount (P, mm), temperature (T, °C), and relative humidity (RH, %) were observed after event precipitation sampling at each observation station. Due to the limitations imposed by field conditions, seven stations with data integrity in 2015 (Figure 1) were selected for analysis in this study. Deuterium excess (d-excess), a second-order parameter that combines both oxygen and hydrogen isotopic species, is defined by the following expression (Dansgaard, 1964): d-excess = $\delta^2H - 8 \times \delta^{18}O$.

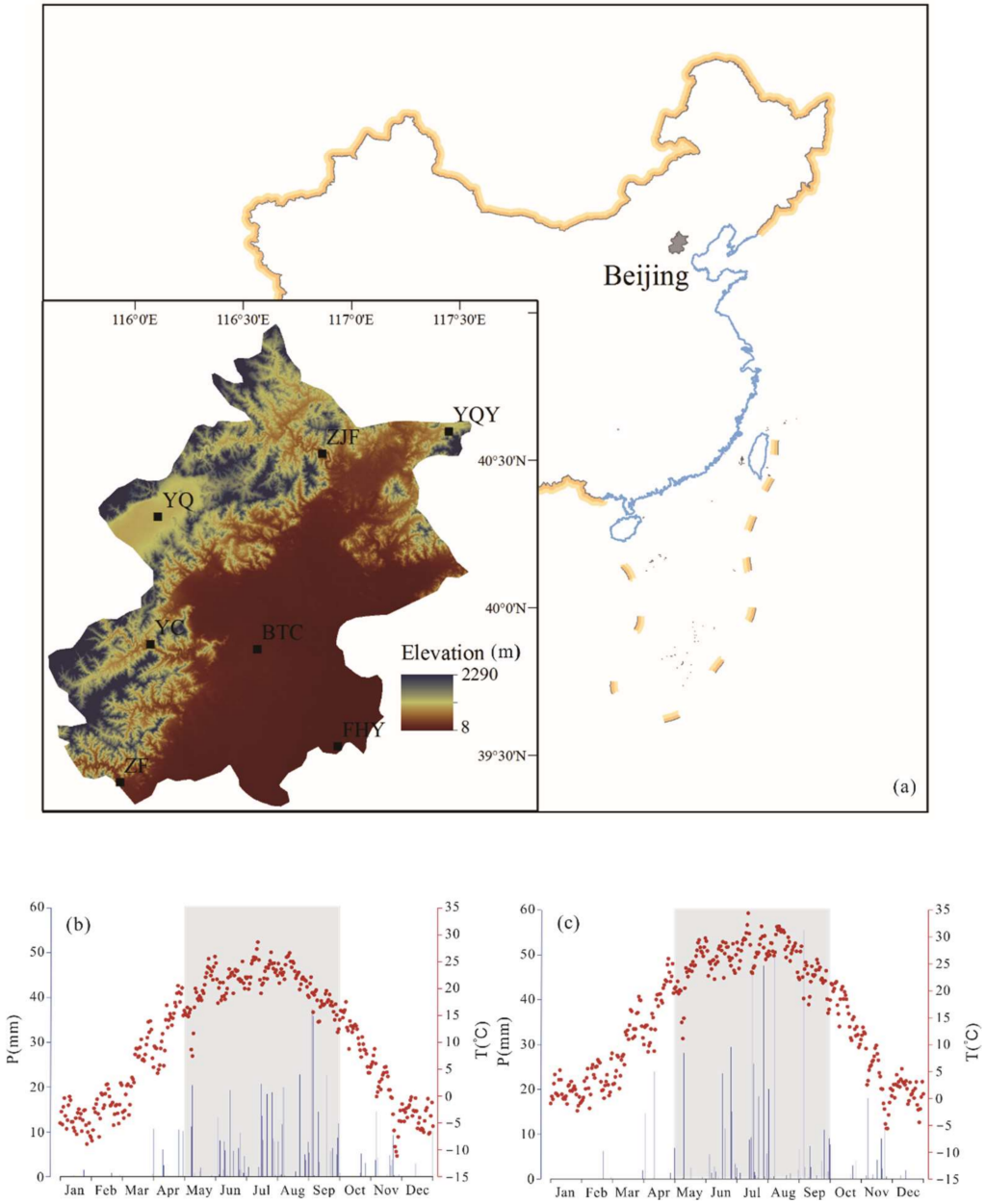

Figure 1. (**a**) Topography and locations of sampling stations for precipitation isotopes over the Beijing region (BNIP). Daily precipitation amount and temperature variations at (**b**) YQ and (**c**) BTC stations during 2015. Data at YQ station were obtained from the China Meteorological Data Sharing Service System (CMDSSS, http://cdc.cma.gov.cn/home.do (accessed on 1 January 2018). BTC station data were collected by the authors for this study. The shaded part in the figure indicates the monsoonal season from May to September. The red points and blue lines represent temperature and precipitation amounts, respectively.

2.3. Moisture Trajectories

To deduce the probable moisture trajectories in the study area, we generated backward trajectories using the Hybrid Single-Particle Lagrangian Integrated Trajectory (HYSPLIT) model, developed by the National Oceanic and Atmospheric Administration (NOAA) Air Resources Laboratory [42]. Three-dimensional wind fields for trajectory calculation were derived from the Global Data Assimilation System (GDAS) of the National Centers for Environmental Prediction (NCEP). The most rainfall in summer over Beijing precipitates from clouds with base heights of 1000–2000 m [43]. Therefore, we used an average height of 1500 m in the HYSPLIT model to obtain the moisture trajectories.

2.4. Spatial Interpolation

Spatial interpolation provides a method for estimating the isotopic compositions of precipitation where data are not available, and a smoothed trend surface is generated that captures the geographic data variability. In this study, the contours of $\delta^{18}O$ and $\delta^{2}H$ values for precipitation over Beijing were mapped using Kriging interpolation in ArcGIS 10.8 software. The surrounding GNIP stations, including Shijiazhuang, Tianjin, Jinzhou, and Changchun, were incorporated to eliminate the boundary effect. We calculated the amount-weighted $\delta^{18}O$ from June to August as summer, and from December to February as winter.

3. Results

3.1. Spatial Distribution of Annual Mean Stable Isotopes in Precipitation

In the observed stations, mean annual $\delta^{18}O$, $\delta^{2}H$, and deuterium excess values ranged from −7.6 to −9.6‰, −51.9 to −65.0‰, and 9.3~11.5‰, respectively (see Table 1). Although the isotopic values were relatively stable, a clear pattern was found: the spatial distribution of $\delta^{18}O$ and $\delta^{2}H$ was almost parallel to the latitude lines (Figure 2a,b), with increasingly negative values at higher (more northern) latitudes, which is in good agreement with the $\delta^{18}O$ precipitation contour map for China [31]. In contrast, the deuterium excess was almost the same over the whole Beijing region.

The spatial variations in $\delta^{18}O$ of precipitation during the summer and winter seasons are shown in Figure 2c,d. During the winter season, the precipitation contours indicated a clear increasing trend from northwest to south. During the summer season, precipitation $\delta^{18}O$ was more enriched, but within a narrow range. We also found that the summer $\delta^{18}O$ values were close to the annual values, likely because precipitation is concentrated in the summer (Figure 1a,c).

Table 1. BNIP station locations, annual precipitation amount, annual mean temperature, and measured annual mean precipitation isotopic values.

Station	Longitude (°E)	Latitude (°N)	Elevation (m)	$\delta^{2}H$ (‰)	$\delta^{18}O$ (‰)	d_{excess} (‰)	P (mm)	T (°C)
YQY	117.375	40.637	477	−57.0	−8.5	11.2	540.8	12.3 *
ZJF	116.782	40.614	186	−59.4	−8.6	9.3	596.1	14.2 *
YQ	115.993	40.463	492	−65.0	−9.6	11.5	531.0	10.2
YC	115.894	40.033	238	−51.9	−7.7	9.3	423.7	15.3 *
FHY	116.694	39.615	11	−58.0	−8.7	11.4	474.1	16.8 *
ZF	115.688	39.576	108	−49.7	−7.6	11.4	514.9	13.5 *
BTC	116.379	39.976	54	−59.7	−8.8	10.3	600.3	15.1

Note. * denotes the average temperature of all the recorded data at the sampling events.

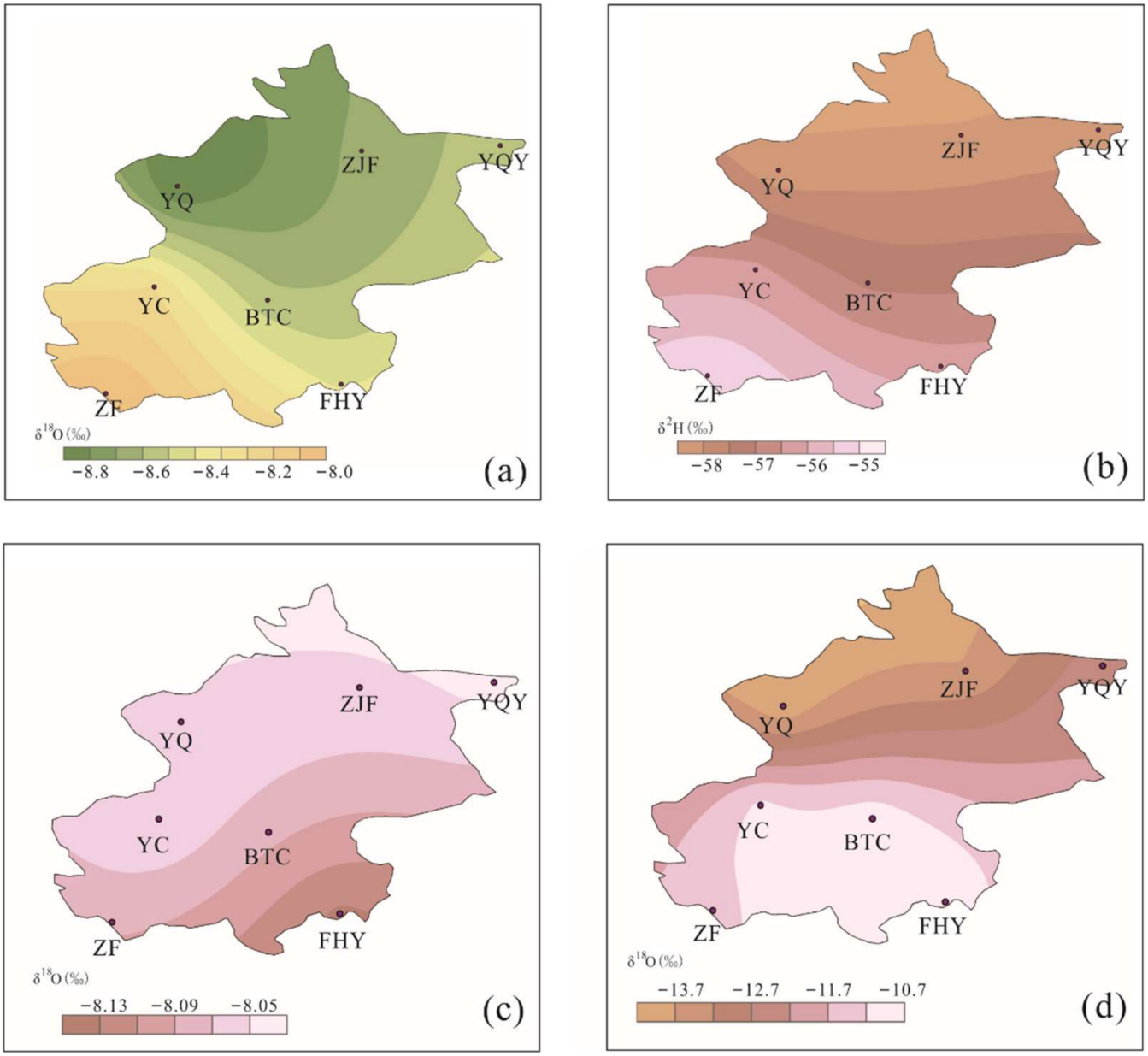

Figure 2. Mean annual gridded values of stable isotopes compositions of meteoric waters over Beijing (**a**) $\delta^{18}O$, (**b**) $\delta^{2}H$, (**c**) $\delta^{18}O$ during summer seasons, and (**d**) $\delta^{18}O$ during winter seasons.

3.2. Seasonal Variations in Precipitation Isotopes

Seasonal changes in $\delta^{18}O$ were similar at all stations (Figure 3a), with a broad maximum, −2.0~−9.5‰ and −19.2~−67.7‰ for $\delta^{18}O$ and $\delta^{2}H$ values, respectively, during the summer months. The minima, −9.1‰~−21.5‰ and −157.6~−45.8‰ for $\delta^{18}O$ and $\delta^{2}H$ values, respectively, occurred in the winter months. Such a seasonal variation was also observed by Wen et al. (2010) [40] for both vapor and precipitation isotopes at a station in Beijing, and by Yamanaka et al. (2004) [30] for multi-year precipitation isotopes in the northern North China Plain.

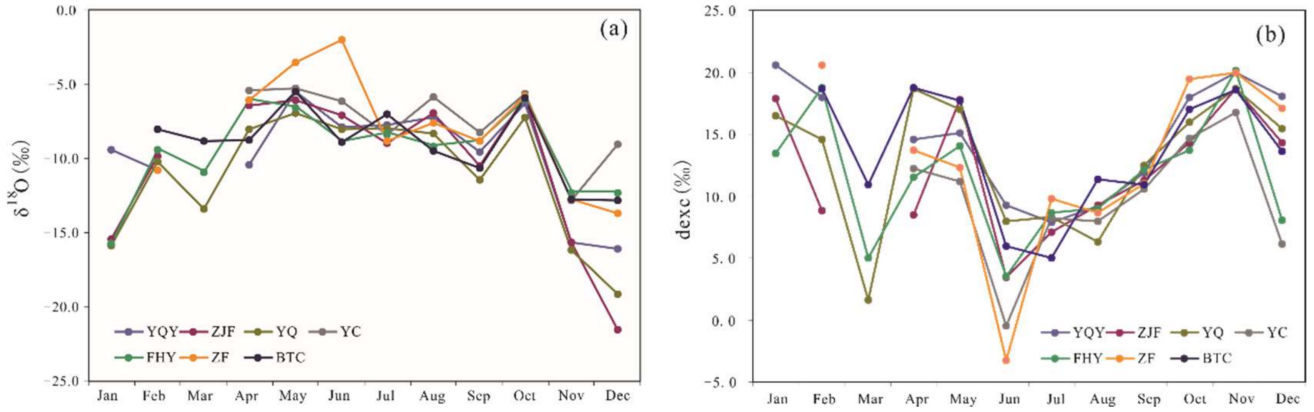

Figure 3. Seasonal variations in (**a**) $\delta^{18}O$ and (**b**) d-excess at seven stations in Beijing in 2015.

Different from the stable isotopes, the annual variations in deuterium excess show a dominant 'V'-shaped pattern in Beijing (Figure 3b). The arrival of the monsoon at these stations was marked by an increase in rainfall (Figure 1b,c), and a corresponding increase (drop) in $\delta^{18}O$ (deuterium excess) values. The much more pronounced minima for $\delta^{18}O$ were observed during the winter months, associated with relatively high d-excess values. These elevated d-excess values indicate the presence of continental air masses producing precipitation during the winter season.

3.3. Local Meteoric Water Line

Isotopic ratios of D/H and $^{18}O/^{16}O$ in precipitation are closely related, lying on a meteoric water line, which provides isotopic input functions for hydrological studies. The local meteoric water line (LMWL) for Beijing (Figure 4), derived from amount-weighted monthly values in this study, was calculated as:

$$\delta^2H = 7.5\delta^{18}O + 8.2 \ (R^2 = 0.97, n = 77) \quad (1)$$

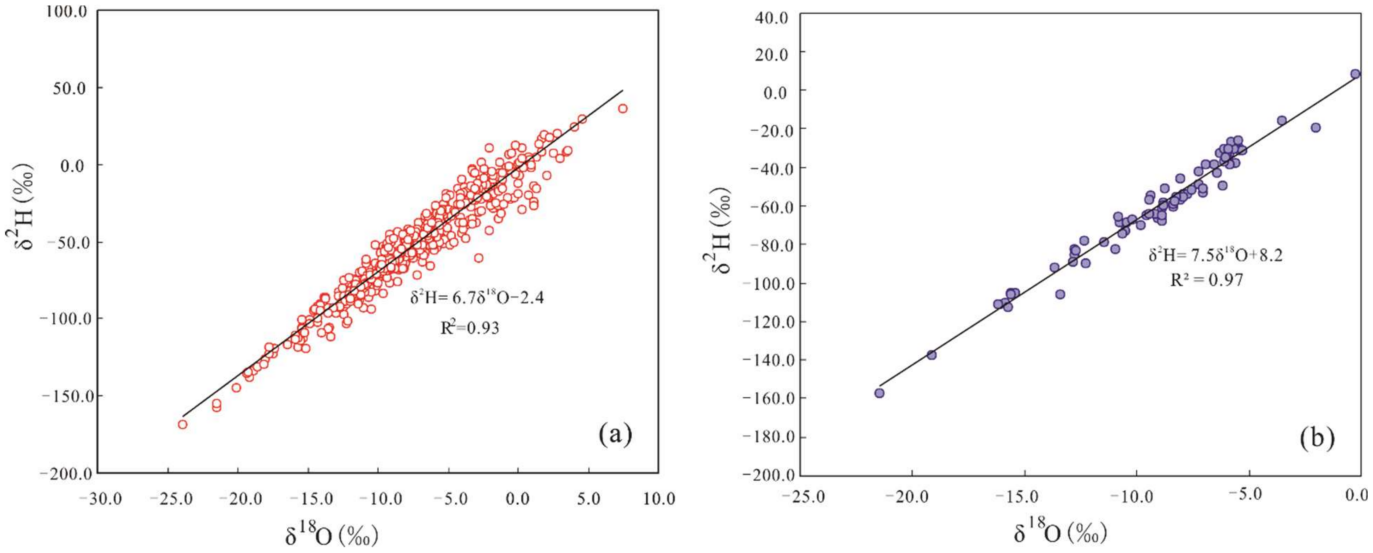

Figure 4. Correlation between δ^2H and $\delta^{18}O$ values for Beijing precipitation in 2015: (**a**) δ^2H and $\delta^{18}O$ values of individual samples (n = 539): $\delta^2H = 6.7\delta^{18}O - 2.4$; and (**b**) monthly amount-weighted average δ^2H and $\delta^{18}O$ values (n = 77): $\delta^2H = 7.5\delta^{18}O + 8.2$.

The slope and intercept of the LMWL increased continuously with increasing P (Table 2). For all the rain events, the slope of the $\delta^2H/\delta^{18}O$ relationship was 6.7, within the range calculated using a numerical secondary evaporation model [44]. When the individual

P was >5 mm, the LMWL based on individual data had a slope close to that based on the monthly weighted data. For the storm events, e.g., ≥10mm, the slope of the $\delta^2H/\delta^{18}O$ relationship was obviously higher at 7.7. Secondary evaporation is always observed for light rain events, or at the beginning of storms in an arid environment [45]. Based on our data from Beijing, the change to precipitation isotopes due to secondary evaporation was most pronounced for rain samples with $P < 0.5$ mm (slope = 6.2).

Table 2. Correlation equations for δ^2H and $\delta^{18}O$ values of individual precipitation samples with different precipitation amount ranges in Beijing, China.

Precipitation AmountRange	$\delta^2H/\delta^{18}O$ Correlation Equations	R^2	N
≥0	$\delta^2H = 6.7\delta^{18}O - 2.4$	0.93	539
≥1.0	$\delta^2H = 7.0\delta^{18}O + 1.1$	0.94	400
≥5.0	$\delta^2H = 7.4\delta^{18}O + 6.4$	0.96	199
≥10.0	$\delta^2H = 7.7\delta^{18}O + 8.9$	0.96	115

4. Discussion

4.1. Relationship between $\delta^{18}O$ and T or P

The regression equation between $\delta^{18}O$ and T or P (the so-called T or P effect of Dansgaard (1964) [46]) was calculated based on both daily and monthly data. For monthly data, a clear relationship between the mean monthly $\delta^{18}O$ and T during the non-monsoonal season is shown in Figure 5a, with a high correlation coefficient (R^2) of 0.74. The $\delta^{18}O/T$ slope was 0.4 ‰/°C, which is in good agreement with that of the typical westerlies domain (Urumqi station in Xinjiang Uygur Autonomous Region as an example). Points from the monsoonal season were plotted below the regression line for T and $\delta^{18}O$. In contrast, the $\delta^{18}O$ during the monsoonal season showed a significant P effect (Figure 5b); the monthly slope was approximately −2.9‰/100 mm (R^2 = 0.53). This agrees with the conclusions of Li et al. (2014) [31] that T and P effects dominate in different seasons.

To demonstrate and interpret the relationship more clearly, daily data from BTC and YQ stations were selected for further evaluation. For daily data, $\delta^{18}O$ only correlated well with T when T was below 16 °C, and the gradient of the T effect at the two stations was similar, with a value of 0.4‰/°C. When T was above 16 °C, the T effect disappeared, as shown by the scattered points indicated with a rectangle in Figure 5c. It should be noted that conditions with T > 16 °C only occur in the monsoon season.

We compared our findings with the results from the Gaoshan and Houxia stations in the Tianshan Mountains (Figure 5c). For all four stations, the T effect only exists within a certain temperature range, below 0 °C for Gaoshan and Houxia stations, and below 16 °C for YQ and BTC stations. However, when there is no T effect, the $\delta^{18}O$ values change very little at Gaoshan and Houxia stations, while they fluctuate remarkably over the Beijing region. The Tianshan Mountains are dominated by westerlies throughout the year, and sub-cloud evaporation and moisture recycling processes alter the $\delta^{18}O$ values when T is above 0 °C [47–50]. The moisture in Beijing is controlled by the westerlies and polar air masses in winter (Figure 6). Similar to other regions with prevailing westerlies, the temperature effect is significant in Beijing during the non-monsoon seasons, as shown in Figure 5a,c. During the monsoon seasons, rain samples reveal a depleted isotope signature despite generally higher summer temperatures. Because $\delta^{18}O$ is affected by the sub-cloud evaporation process when P is small, the heavy daily rainfall events (>5 mm/day) from YQ and BTC stations are clustered. A significant inverse relationship between $\delta^{18}O$ and P is observed (Figure 5d). When the moisture sources at BTC station are limited to from the south and west (northwest) based on HYSPLIT trajectories, R^2 increases to 0.53 and 0.49, respectively, illustrating more significant correlations, which also imply the significant effect of rainfall sources on precipitation $\delta^{18}O$ to some extent.

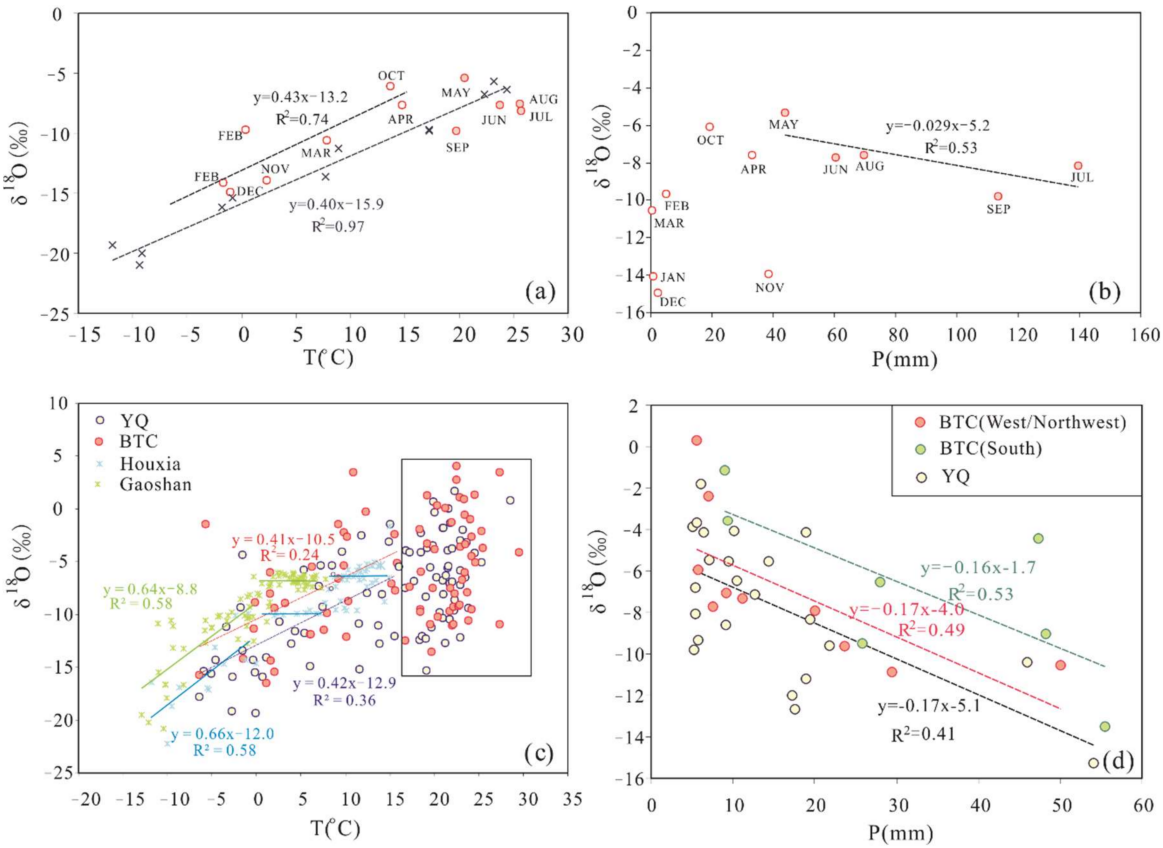

Figure 5. Correlation between monthly amount-weighted average $\delta^{18}O$ values of samples and (**a**) T and (**b**) P. The filled points are samples from the monsoonal season, and the empty circles are samples during the non-monsoon seasons; the blue points are data from Urumqi station, where westerlies are the only advected moisture source. $\delta^{18}O$ changes with (**c**) temperature and (**d**) P at the BTC and YQ stations. Only *P* with >5 mm/day was selected in Figure 5d. Directional labels indicate the source regions for the moisture.

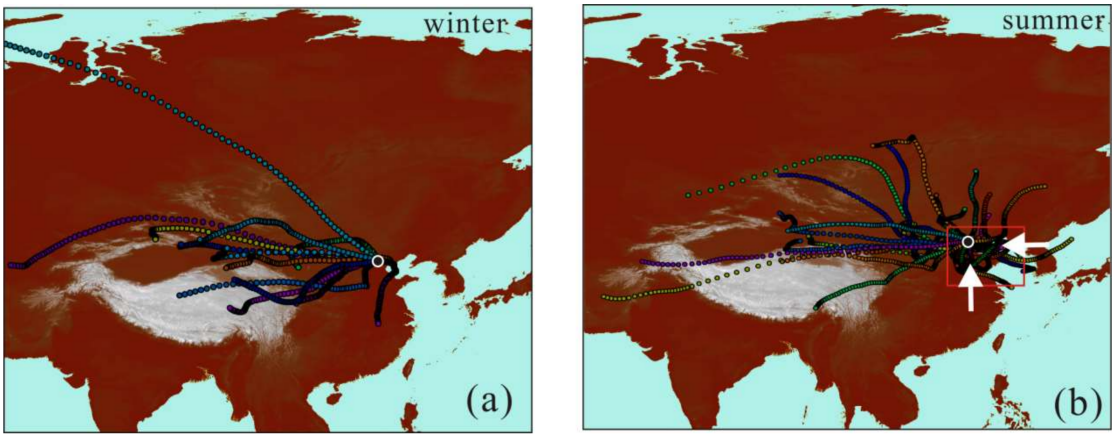

Figure 6. Moisture trajectories obtained from the HYSPLIT model through the layer from the surface to 1500 m for 72 h at the beginning of precipitation during the (**a**) winter and (**b**) summer seasons. The white point indicates BTC station. The rectangle covers the moisture trajectories from south and east.

4.2. Moisture Sources over the Beijing Region

The moisture sources affecting Beijing are composed of both continental moisture from the northwest and marine moisture from the south. However, their contributions

to the Beijing vapor each month are quite different. The HYSPLIT model was used to show moisture trajectories for the study period over the Beijing region. During the winter season, the moisture was primarily sourced from the northwest; during the summer season, more moisture was transported from the south and east. When we selected rainfall events with $P > 20$ mm to illustrate their trajectories, most were sourced from the south and east (Figure 6).

The isotopes incorporated in continental moisture from the northwest are generally more depleted in heavy isotopes and have higher deuterium excess values than those in marine moisture from the southwest [33]). This is consistent with the spatial patterns illustrated by our data in Figure 2, and the seasonal pattern illustrated in Figure 3. To understand the effect of moisture sources on the precipitation isotopes, a Rayleigh distillation model [7] was employed based on continuously selected daily data from 16–20 July 2015.

Figure 7 displays the isotopic variations during rainfall events at seven stations. A decreasing isotopic trend was observed during the first four days, in good agreement with the Rayleigh distillation model. However, an increasing trend for isotopes was observed on 20 July 2015 with the addition of a new air mass. The increasing isotopic compositions were first found at BTC, ZF, and YC stations, indicating a southwestern moisture source. This is in agreement with the HYSLTIP results shown in Figure 8. Moisture extended from offshore areas westward over Beijing during the first four days, while air from further inland contributed more to rainfall on 20 July 2015.

Initially, the moisture derived from offshore areas (initial moisture) arrived in Beijing from east to west (Figure 8b). The $\delta^{18}O$ value of the initial moisture could be obtained from the precipitation $\delta^{18}O$ and corresponding P using an inverse analysis in the Rayleigh fractionation model. For this purpose, we assumed there was no extra moisture added; thus, the initial isotopic values can be calculated using the following two equations:

$$\delta^{18}O_{rain(f)} \approx \delta^{18}O_{(v)} + \varepsilon^{18}O_{l-v} \approx \delta_o^{18}O_v + \varepsilon^{18}O_{l-v} \times \ln f + \varepsilon^{18}O_{l-v} \quad (2)$$

$$f = 1 - \frac{P}{P_{sum}} \quad (3)$$

where $\varepsilon^{18}O_{l-v}$ is 9.3‰ assuming that the temperature is ~25 °C. Using P and $\delta^{18}O$ values for the first two days, the initial isotopic values were calculated, as shown in Figure 9a. Increasingly negative values at higher (more westward) longitudes were obtained with a good correlation coefficient of 0.88 to which is in good agreement with the meteorological results from the HYSPLIT models. The initial $\delta^{18}O$ value for the YQY station was about −0.6‰, similar to that of seawater [51] which provided further evidence for an eastern moisture source from offshore. There was no remarkable difference in isotopes on 19 July, and the decreasing isotopic trend (Figure 9b) from south to north for the rainfall on 20 July was primarily caused by the southern moisture sources, with a negligible P effect. New southern air masses, mainly derived from terrestrial evaporation, were more enriched compared to isotopes of residual moisture. Therefore, precipitation $\delta^{18}O$ was mainly controlled by the initial isotopic values, residual vapor fraction, and input of new air masses. The initial isotopic values were again dominated by moisture source and rainout process before arriving at the rainfall location, and the input of new air masses should be seen as a moisture source factor. Therefore, moisture sources and residual vapor fraction during the rainout process dominated the rhythm of $\delta^{18}O$ in the monsoon-affected region of Beijing.

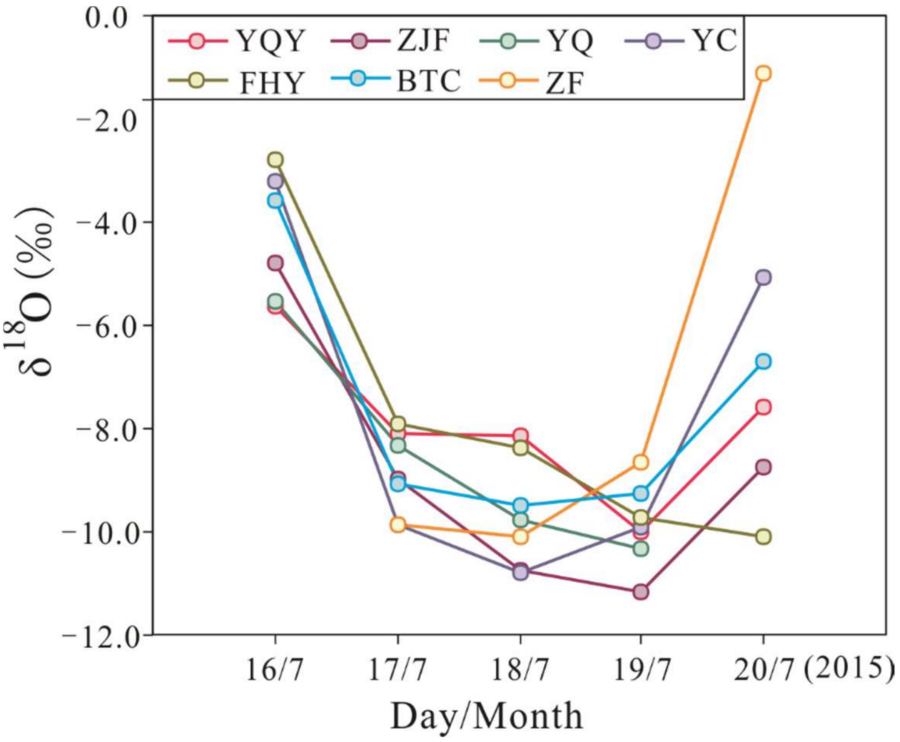

Figure 7. The isotopic variations in continuous precipitation events at seven stations over the Beijing region.

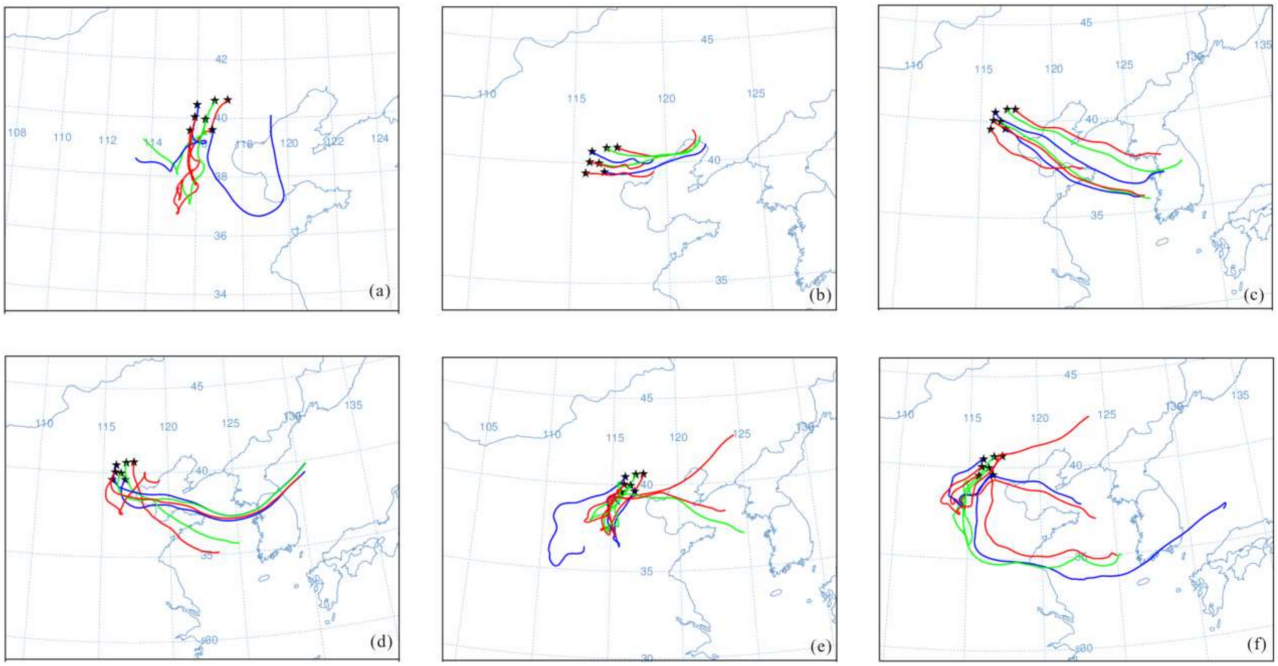

Figure 8. Moisture trajectories obtained using the HYSPLIT model through the layer from the surface to 1500 m for 48 h at 08:00 Beijing Time on (**a**) 15 July, (**b**) 16 July, (**c**) 17 July, (**d**) 18 July, (**e**) 19 July, and (**f**) 20 July.

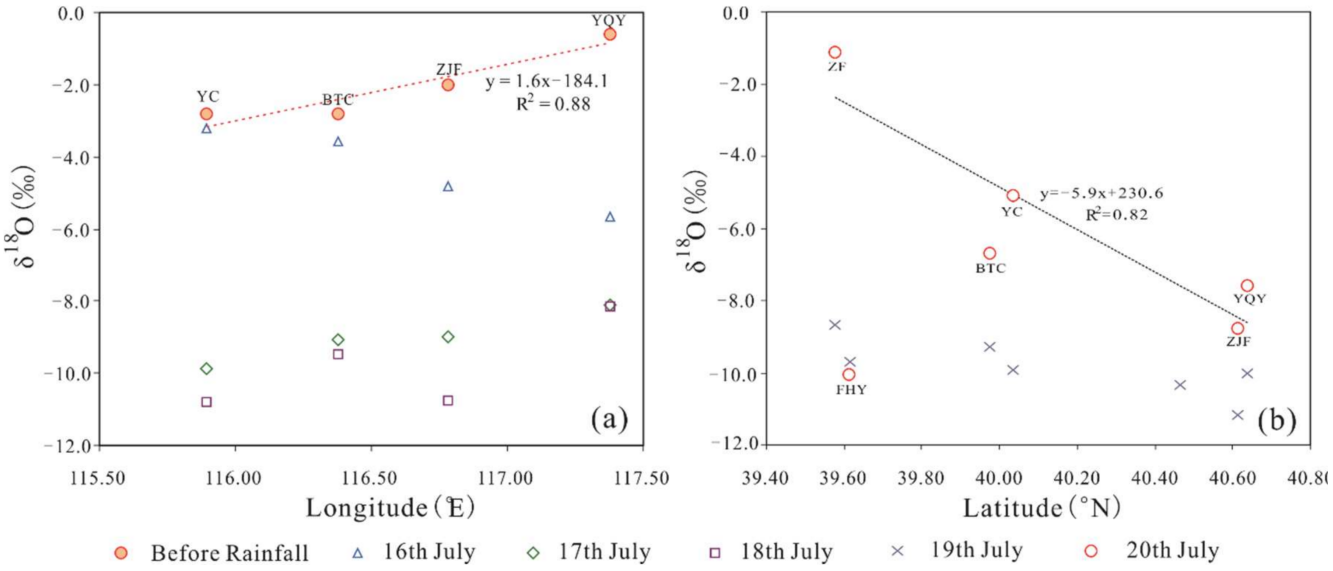

Figure 9. The plot of $\delta^{18}O$ versus (**a**) longitude and (**b**) latitude for continuous precipitation events at seven stations.

5. Conclusions

Daily precipitation samples were collected throughout 2015 and analyzed from seven stations covering the mountain and basin region of Beijing. The dominant factors controlling $\delta^{18}O_p$ and changes in $\delta^{18}O_p$ related to temperature and precipitation variabilities in the monsoon-affected region were identified.

The annual $\delta^{18}O_p$ and $\delta^{2}H_p$ show a clear spatial pattern that increases from south (east) to north (west), while the deuterium excess varies little. The summer $\delta^{18}O_p$ is relatively stable, while the winter $\delta^{18}O_p$ increases from northwest to south. Such a spatial distribution feature is mainly controlled by northwest continental and south marine moisture sources. The seasonal changes in $\delta^{18}O$ are very similar at all stations, with high values in summer and low values in winter. Both the high $\delta^{18}O$ values and low deuterium excess values from May to September reveal the impact of the monsoon. The local meteoric water line (LMWL) for Beijing, derived from amount-weighted monthly values is $\delta^{2}H = 7.5\ \delta^{18}O + 8.2$ ($R^2 = 0.97$, $n = 77$). The smaller slope of 6.7 derived from individual events is attributed to a local secondary evaporation process. A significant T effect is found, with a gradient of 0.4‰/°C when T is below 16 °C. In the monsoon season, when T is always above 16 °C, the P effect dominates, particularly when $P > 5$ mm.

A Rayleigh distillation model was employed to verify the factors controlling the precipitation isotopes based on selected continuous event data for 16–20 July 2015. We found that the moisture sources and residual vapor fraction are the most important factors controlling the rhythm of $\delta^{18}O$. The limited observed period from these stations is recognized, and an extension of such isotopic studies over a longer period, and the inclusion of more stations will obtain more quantitative determination of the various effects on the formation of precipitation in the monsoon-affected region.

Author Contributions: Conceptualization, J.L. and Z.P.; investigation, G.B. and H.Z.; writing—original draft, J.L.; writing—review and editing, Z.P. and L.T. All authors have read and agreed to the published version of the manuscript.

Funding: This work was supported by the National Natural Science Foundation of China (41372257, 41602276, and 42106228), a China Postdoctoral Science Foundation Funded Project (2015M581168), and the CRP projects of IAEA (No. F33024 and F31006).

Institutional Review Board Statement: Not applicable.

Informed Consent Statement: Not applicable.

Data Availability Statement: All data used during the study are available from the corresponding author by request.

Acknowledgments: This paper is dedicated to the memory of Klaus Froehlich, former Head of the Isotope Hydrology Section of the International Atomic Energy Agency (IAEA), who guided our study on isotopes in precipitation. We are grateful to Ming Tan for giving insightful suggestions to improve the manuscript. We sincerely appreciate the staff members of all the hydrology observatory stations for their assistance in collecting the precipitation samples.

Conflicts of Interest: The authors declare no conflict of interest.

References

1. Aeschbach-Heritg, W.; Peeters, F.; Beyerle, U.; Kipfer, R.P. Palaeotemperature reconstruction from noble gases in ground water taking into account equilibration with entrapped air. *Nature* **2000**, *405*, 1040–1044. [CrossRef] [PubMed]
2. McDermott, F.; Mattey, D.P.; Hawkesworth, C. Centennial-scale holocene climate variability revealed by a high-resolution speleothem d18O record from SW Ireland. *Science* **2001**, *294*, 1328–1331. [CrossRef] [PubMed]
3. Wang, Y.J.; Cheng, H.; Edwards, R.L.; An, Z.S.; Wu, J.Y.; Shen, C.-C.; Dorale, J.A. A High-Resolution Absolute-Dated Late Pleistocene Monsoon Record from Hulu Cave, China. *Science* **2001**, *294*, 2345–2348. [CrossRef]
4. Hu, C.; Henderson, G.M.; Huang, J.; Xie, S.; Sun, Y.; Johnson, K.R. Quantification of Holocene Asian monsoon rainfall from spatially separated cave records. *Earth Planet. Sci. Lett.* **2008**, *266*, 221–232. [CrossRef]
5. Williams, P.P.W.; Fowler, A. Relationship between oxygen isotopes in rainfall, cave percolation waters and speleothem calcite at Waitomo, New Zealand. *J. Hydrol. New. Zeal.* **2002**, *41*, 53–70.
6. McDermott, F. Palaeo-climate reconstruction from stable isotope variations in speleothems: A review. *Quat. Sci. Rev.* **2004**, *23*, 901–918. [CrossRef]
7. Clark, I.D.; Fritz, P. *Environmental Isotopes in Hydrogeology*, 2nd ed.; CRC Press: New York, NY, USA, 1997; pp. 13–168. ISBN 978 1 5667 0249 2. [CrossRef]
8. Edmunds, W.; Ma, J.; Aeschbach-Hertig, W.; Kipfer, R.; Darbyshire, D. Groundwater recharge history and hydrogeochemical evolution in the Minqin Basin, North West China. *Appl. Geochem.* **2006**, *21*, 2148–2170. [CrossRef]
9. Beyerle, U. Evidence for periods of wetter and cooler climate in the Sahel between 6 and 40 kyr BP derived from groundwater. *Geophys. Res. Lett.* **2003**, *30*, 1173–1177. [CrossRef]
10. Chen, Z.J.; Qi, J.; Xu, J.; Xu, J.; Ye, H.; Nan, Y. Paleoclimatic interpretation of the past 30 ka from isotopic studies of the deep confined aquifer of the North China plain. *Appl. Geochem.* **2003**, *18*, 997–1009.
11. Li, J.; Pang, Z.; Froehlich, K.; Huang, T.; Kong, Y.; Song, W.; Yun, H. Paleo-environment from isotopes and hydrochemistry of groundwater in East Junggar Basin, Northwest China. *J. Hydrol.* **2015**, *529*, 650–661. [CrossRef]
12. Kreuzer, A.M.; von Rohden, C.; Friedrich, R.; Chen, Z.; Shi, J.; Hajdas, I.; Kipfer, R.; Aeschbach-Hertig, W. A record of temperature and monsoon intensity over the past 40 kyr from groundwater in the North China Plain. *Chem. Geol.* **2009**, *259*, 168–180. [CrossRef]
13. Neff, U.; Burns, S.J.; Mangini, A.; Mudelsee, M.; Fleitmann, D.; Matter, A. Strong coherence between solar variability and the monsoon in Oman between 9 and 6 kyr ago. *Nature* **2001**, *411*, 290–293. [CrossRef] [PubMed]
14. Fleitmann, D.; Burns, S.J.; Mudelsee, M.; Neff, U.; Kramers, J.; Mangini, A.; Matter, A. Holocene Forcing of the Indian Monsoon Recorded in a Stalagmite from Southern Oman. *Science* **2003**, *300*, 1737–1739. [CrossRef] [PubMed]
15. Baker, A.; Asrat, A.; Fairchild, I.J.; Leng, M.J.; Wynn, P.M.; Bryant, C.; Genty, D.; Umer, M. Analysis of the climate signal contained within δ18O and growth rate parameters in two Ethiopian stalagmites. *Geochim. Cosmochim. Acta* **2007**, *71*, 2975–2988. [CrossRef]
16. Wang, Y.; Cheng, H.; Edwards, R.L.; Kong, X.; Shao, X.; Chen, S.; Wu, J.; Jiang, X.; Wang, X.; An, Z. Millennial- and orbital-scale changes in the East Asian monsoon over the past 224,000 years. *Nature* **2008**, *451*, 1090–1093. [CrossRef]
17. Yuan, D.; Cheng, H.; Edwards, R.L.; Dykoski, C.A.; Kelly, M.J.; Zhang, M.; Qing, J.; Lin, Y.; Wang, Y.; Wu, J.; et al. Timing, Duration, and Transitions of the Last Interglacial Asian Monsoon. *Science* **2004**, *304*, 575–578. [CrossRef]
18. Cheng, H.; Edwards, R.L.; Broecker, W.S.; Denton, G.H.; Kong, X.; Wang, Y.; Zhang, R.; Wang, X. Ice age terminations. *Science* **2009**, *326*, 248–252. [CrossRef]
19. Cruz, F.; Burns, S.; Karmann, I.; Sharp, W.; Vuille, M. Reconstruction of regional atmospheric circulation features during the late Pleistocene in subtropical Brazil from oxygen isotope composition of speleothems. *Earth Planet. Sci. Lett.* **2006**, *248*, 495–507. [CrossRef]
20. Maher, B. Holocene variability of the East Asian summer monsoon from Chinese cave records: A re-assessment. *Holocene* **2008**, *18*, 861–866. [CrossRef]
21. LeGrande, A.N.; Schmidt, G.A. Sources of Holocene variability of oxygen isotopes in paleoclimate archives. *Clim. Past* **2009**, *5*, 441–455. [CrossRef]

22. Clemens, S.C.; Prell, W.L.; Sun, Y. Orbital-scale timing and mechanisms driving Late Pleistocene Indo-Asian summer monsoons: Reinterpreting cave speleothem $\delta^{18}O$. *Paleoceanography* **2010**, *25*, PA4207. [CrossRef]
23. Dayem, K.E.; Molnar, P.; Battisti, D.S.; Roe, G.H. Lessons learned from oxygen isotopes in modern precipitation applied to interpretation of speleothem records of paleoclimate from eastern Asia. *Earth Planet. Sci. Lett.* **2010**, *295*, 219–230. [CrossRef]
24. Bar-Matthews, M.; Ayalon, A.; Matthews, A.; Sass, E.; Halicz, L. Carbon and oxygen isotope study of the active water-carbonate system in a karstic Mediterranean cave: Implications for paleoclimate research in semiarid regions. *Geochim. Cosmochim. Acta* **1996**, *60*, 337–344. [CrossRef]
25. Taylor, R.G.; Howard, K.W. Groundwater recharge in the Victoria Nile basin of east Africa: Support for the soil moisture balance approach using stable isotope tracers and flow modelling. *J. Hydrol.* **1996**, *180*, 31–35. [CrossRef]
26. Jones, I.C.; Banner, J.L.; Humphrey, J.D. Estimating recharge in a tropical Karst Aquifer. *Water Resour. Res.* **2000**, *36*, 1289–1299. [CrossRef]
27. Jones, I.C.; Banner, J.L. Estimating recharge thresholds in tropical karst island aquifers: Barbados, Puerto Rico and Guam. *J. Hydrol.* **2003**, *278*, 131–143. [CrossRef]
28. Li, J.; Pang, Z.; Kong, Y.; Wang, S.; Bai, G.; Zhào, H.; Zhou, N.; Sun, F.; Yang, Z. Groundwater Isotopes Biased Toward Heavy Rainfall Events and Implications on the Local Meteoric Water Line. *J. Geophys. Res. Atmos.* **2018**, *123*, 6259–6266. [CrossRef]
29. Pape, J.R.; Banner, J.L.; Mack, L.E.; Musgrove, M.; Guilfoyle, A. Controls on oxygen isotope variability in precipitation and cave drip waters, central Texas, USA. *J. Hydrol.* **2010**, *385*, 203–215. [CrossRef]
30. Yamanaka, T.; Shimada, J.; Hamada, Y.; Tanaka, T.; Yang, Y.; Zhang, W.; Hu, C. Hydrogen and oxygen isotopes in precipitation in the northern part of the North China Plain: Climatology and inter-storm variability. *Hydrol. Process.* **2004**, *18*, 2211–2222. [CrossRef]
31. Li, J.; Pang, Z.; Kong, Y.; Zhou, M.; Huang, T. Contrasting seasonal distribution of stable isotopes and deuterium excess in precipitation over China. *Geophys. Res. Lett.* **2014**, *23*, 2078–2085.
32. Liu, J.; Song, X.; Yuan, G.; Sun, X.; Yang, L. Stable isotopic compositions of precipitation in China. *Tellus B Chem. Phys. Meteorol.* **2014**, *66*. [CrossRef]
33. Araguás-Araguás, L.; Froehlich, K.; Rozanski, K. Stable isotope composition of precipitation over southeast Asia. *J. Geophys. Res. Earth Surf.* **1998**, *103*, 28721–28742. [CrossRef]
34. Johnson, K.R.; Ingram, B. Spatial and temporal variability in the stable isotope systematics of modern precipitation in China: Implications for paleoclimate reconstructions. *Earth Planet. Sci. Lett.* **2004**, *220*, 365–377. [CrossRef]
35. Tan, M. Circulation effect: Response of precipitation δ18O to the ENSO cycle in monsoon regions of China. *Clim. Dyn.* **2013**, *42*, 1067–1077. [CrossRef]
36. Allen, S.T.; Keim, R.F.; McDonnell, J.J. Spatial patterns of throughfall isotopic composition at the event and seasonal timescales. *J. Hydrol.* **2014**, *522*, 58–66. [CrossRef]
37. Li, J.; Pang, Z. The elevation gradient of stable isotopes in precipitation in the eastern margin of Tibetan Plateau. *Sci. China Earth Sci.* **2022**, 1–13. [CrossRef]
38. Sun, C.; Tian, L.; Shanahan, T.M.; Partin, J.W.; Gao, Y.; Piatrunia, N.; Banner, J. Isotopic variability in tropical cyclone precipitation is controlled by Rayleigh distillation and cloud microphysics. *Commun. Earth Environ.* **2022**, *3*, 1–10. [CrossRef]
39. Li, J.; Tao, T.; Pang, Z.; Tan, M.; Kong, Y.; Duan, W.; Zhang, Y. Identification of Different Moisture Sources through Isotopic Monitoring during a Storm Event. *J. Hydrometeorol.* **2015**, *16*, 1918–1927. [CrossRef]
40. Wen, F.X.; Zhang, S.C.; Sun, X.M.; Yu, G.R.; Lee, X. Water vapor and precipitation isotope ratios in Beijing, China. *JGR Atmos.* **2010**, *115*, D01103. [CrossRef]
41. Zhai, Y.; Wang, J.; Zhang, Y.; Teng, Y.; Zuo, R.; Huan, H. Hydrochemical and isotopic investigation of atmospheric precipitation in Beijing. *China. Sci. Total Environ.* **2013**, *456–457*, 202–211. [CrossRef]
42. Draxler, R.; Rolph, G. HYbrid single-particle lagrangian integrated trajectory (HYSPLIT) 2003. Available online: http://www.arl.noaa.gov/ready/hysplit4.html (accessed on 20 July 2022).
43. Shang B, Zhou Y, Liu J, Huang Y Comparing vertical structure of precipitation cloud and non-precipitation cloud using Cloudsat. *J. Appl. Meteorol. Sci.* **2012**, *23*, 1–9.
44. Salamalikis, V.; Argiriou, A.; Dotsika, E. Isotopic modeling of the sub-cloud evaporation effect in precipitation. *Sci. Total Environ.* **2016**, *544*, 1059–1072. [CrossRef] [PubMed]
45. Kong, Y.; Pang, Z. A positive altitude gradient of isotopes in the precipitation over the Tianshan Mountains: Effects of moisture recycling and sub-cloud evaporation. *J. Hydrol.* **2016**, *542*, 222–230. [CrossRef]
46. Dansgaard, W. Stable Isotopes in Precipitation. *Tellus* **1964**, *16*, 436–468. [CrossRef]
47. Tian, L.; Yao, T.; MacClune, K.; White, J.W.C.; Schilla, A.; Vaughn, B.; Vachon, R.; Ichiyanagi, K. Stable isotopic variations in west China: A consideration of moisture sources. *J. Geophys. Res. Earth Surf.* **2007**, *112*. [CrossRef]
48. Pang, H.Z.; Kong, Y.L.; Froehlich, K.; Huang, T.M.; Yuan, L.J.; Li, Z.Q.; Wang, F.T. Processes affecting isotopes in precipitation of an arid region. *Tellus B* **2011**, *63*, 352–359. [CrossRef]
49. Wang, S.; Zhang, M.; Che, Y.; Chen, F.; Qiang, F. Contribution of recycled moisture to precipitation in oases of arid central Asia: A stable isotope approach. *Water Resour. Res.* **2016**, *52*, 3246–3257. [CrossRef]

50. Kong, Y.; Pang, Z.; Froehlich, K. Quantifying recycled moisture fraction in precipitation of an arid region using deuterium excess. *Tellus B: Chem. Phys. Meteorol.* **2013**, *65*. [CrossRef]
51. LeGrande, A.N.; Schmidt, G.A. Global gridded data set of the oxygen isotopic composition in seawater. *Geophys. Res. Lett.* **2006**, *33*. [CrossRef]